Abstract

In the northern Yamato Mountains, there are two groups of rocks. One is the syenite gneiss group which was metamorphosed under the granulite facies conditions. The other is the granite gneiss group which was metamorphosed under the amphibolite facies conditions. Besides, metabasites and acid dykes are found to accompany them.

There is gradational transition between the two groups of the rocks, and it is revealed from the field and microscopic observations that the transition is not progressive metamorphism but the early-formed syenite gneiss was activated under the amphibolite facies conditions resulting in the granite gneiss.

According to the bulk chemical analysis the trend of the granitization in the diagram, norm q-or-ab-ne, is characterized by the decrease of "or" and the increase of "q". Finally the point of eutectic minimum is reached. Therefore, it seems evident that the granitization occurred in association with anatexis.

1. Introduction

The Yamato Mountains, situated at about 300 km southwest of Syowa Station of Ongul Islands, are representative of the mountains fringing the East Antarctic Continent (Fig. 1).

The geological investigation of the Yamato Mountains was first carried out by KIZAKI, a member of the fourth Japanese Antarctic Research Expedition (JARE-4) (1959–61), who compiled a geologic map of the area (1/100,000 in scale) (KIZAKI, 1965). Subsequently, the petrographic studies and further field investigations were carried out (OHTA and KIZAKI, 1966; YOSHIDA and ANDO, 1970). A summarized report of the Yamato Mountains was published, including the Lützow-Holmbukta region (TATSUMI *et al.*, 1964; TATSUMI and KIZAKI,

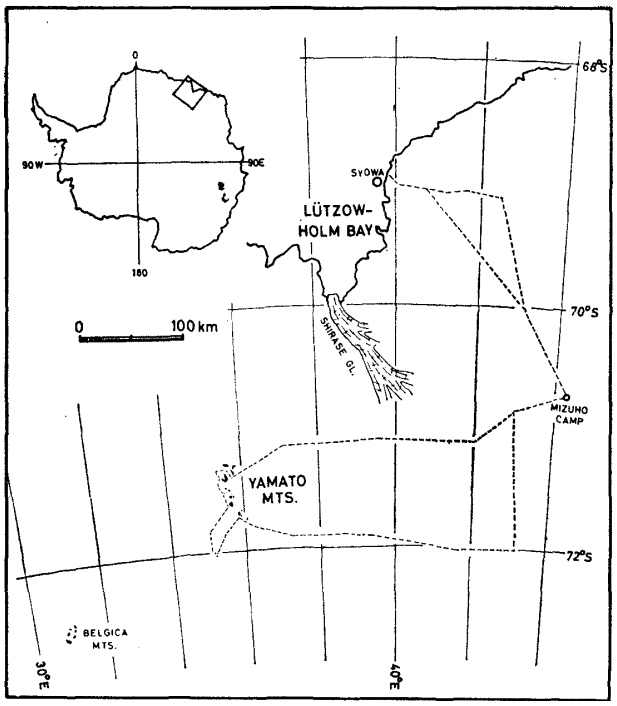

Fig. 1 Location map of the studied area.

1969).

The aim of this study is to describe the geology and petrography of the northern part of the Yamato Mountains and to elucidate the metamorphic history of the rocks involved. Especially in this study, the author tries to clarify the relation between the two major rock groups and to examine the process of granitization.

Field survey was carried out during the author's stay at Syowa Sation as a member of the JARE-14 in 1973. Since a detailed geomorphological map is not available, field data are plotted onto the conventional map modified by air photographs.

2. Geomorphology and Surface Geology

The Yamato Mountains composed of seven massifs and associated nunataks are arranged from north to south for 50 km from 71°17′S, 35°31′E to 71°47′S, 36° 12′ E (Fig. 1). The seven massifs are called provisionally A, B, C, D, E, F and G from south to north and they form an arc convex to the west. A group of nunataks continues northeastwards from the southern end of Massif A.

The outline of the regional geomorphology has been discussed by YOSHIDA and FUJIWARA (1963). In this section some conspicuous features of the surveyed area will be described.

The greater part of the ice-free area is covered with morainic debris but the rocks are well exposed in the cliffs along the margin of the massifs and nunataks. Comparatively gentle slopes develop in Massifs D, E and F. In Massif D, three different levels of planes are clearly recognized. This fact indicates that the retrogression of the ice sheet occurred in three stages. In Massif E, a typical U-shaped valley is found at the level of 100 m above the present ice sheet. Massif G and the southern part of Massif D are made up by the "aiguille".

All of the exposures more or less suffered mechanical weathering. Joint-like cracks and exfoliations parallel to the surface of the exposures are well developed.

Towards the downstream of the massifs, moraine fields spread out with a characteristic fan-like pattern on the ice sheet. A few meters high wavy relief of the moraine (ogive) is developed at a right angle to the direction of the ice flow.

The feature of the ice sheet is contrastive between the both sides of the mountains. The ice sheet flows from east to west in the surveyed area, and katabatic wind blows also from east to west. Thus, on the eastern side of the mountains, a thick snow drift accumulates and a deep wind scoop, 50 m in depth, is formed at the windward foot of the mountains. On the other hand, the bared ice field spreads on the western side of the mountains. Crevasses and ice falls are dominant in the outlet glaciers between the massifs.

The contour map of the basement elevation of the surveyed area is shown in Fig. 2 on the basis of the data measured by radio echo sounder (SHIMIZU *et al.*, 1972; unpublished data by YOKOYAMA). In the figure, it is conspicuous that a

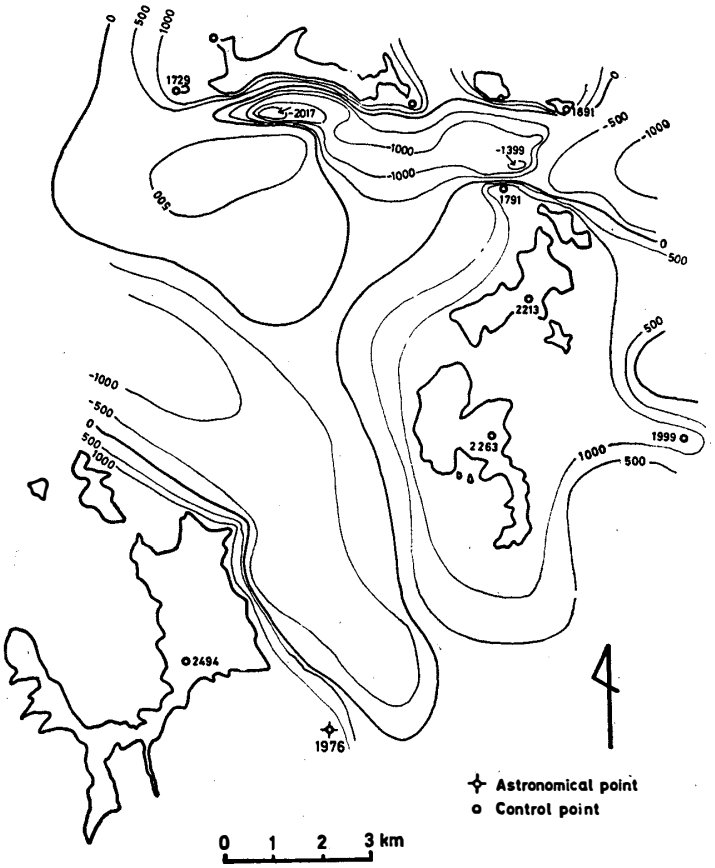

Fig. 2 Subsurface topographical map of the northern Yamato Mountains.

deep trough reaching –2000 m below the sea level is shown along the southern side of Massif G. It is considered to have been produced not merely by glaciation but by structural disturbance such as faulting.

3. Geology

The rocks in the area investigated are classified from the field occurrence as follows. The rock group named charnockitic group by KIZAKI (1965) is defined as syenite gneiss group from its mineral composition. Geologic map of the area is shown in Fig. 3.

1. Syenite gneiss group
   a. Two-pyroxene syenite gneiss
   b. Clinopyroxene syenite gneiss
   c. Clinopyroxene quartz syenite gneiss
2. Granite gneiss group
   a. Granite gneiss
      a-1. Nebulite gneiss
      a-2. Schlieren gneiss
      a-3. Banded gneiss
   b. Migmatite gneiss
      b-1. Biotite granite
      b-2. Two-pyroxene biotite plagioclase gneiss
   c. Aplitic granite
3. Metabasites
4. Acid dyke

3. 1. Syenite gneiss group

The syenite gneiss group is found at Massifs E, F and G and also at small nunataks east of Massif D. The rocks are coarse and rather massive in appearance, and are intercalated with harmonic metabasite bands of 5–20 cm wide. Aplite veins of 5–20 cm are commonly found throughout the syenite gneiss group.

3.1.1. Two-pyroxene syenite gneiss

Massif G and the central parts of Massifs E and F are constructed of two-pyroxene syenite gneiss which represents coarse and melanocratic rocks characterized by the presence of porphyroblasts (0.6–3.0 cm) of dark grey potash feldspar of hypidiomorphic to ellipsoidal form (Fig. 14). The porphyroblasts sometimes show schiller reflection. Foliation is usually obscure but can be recognized

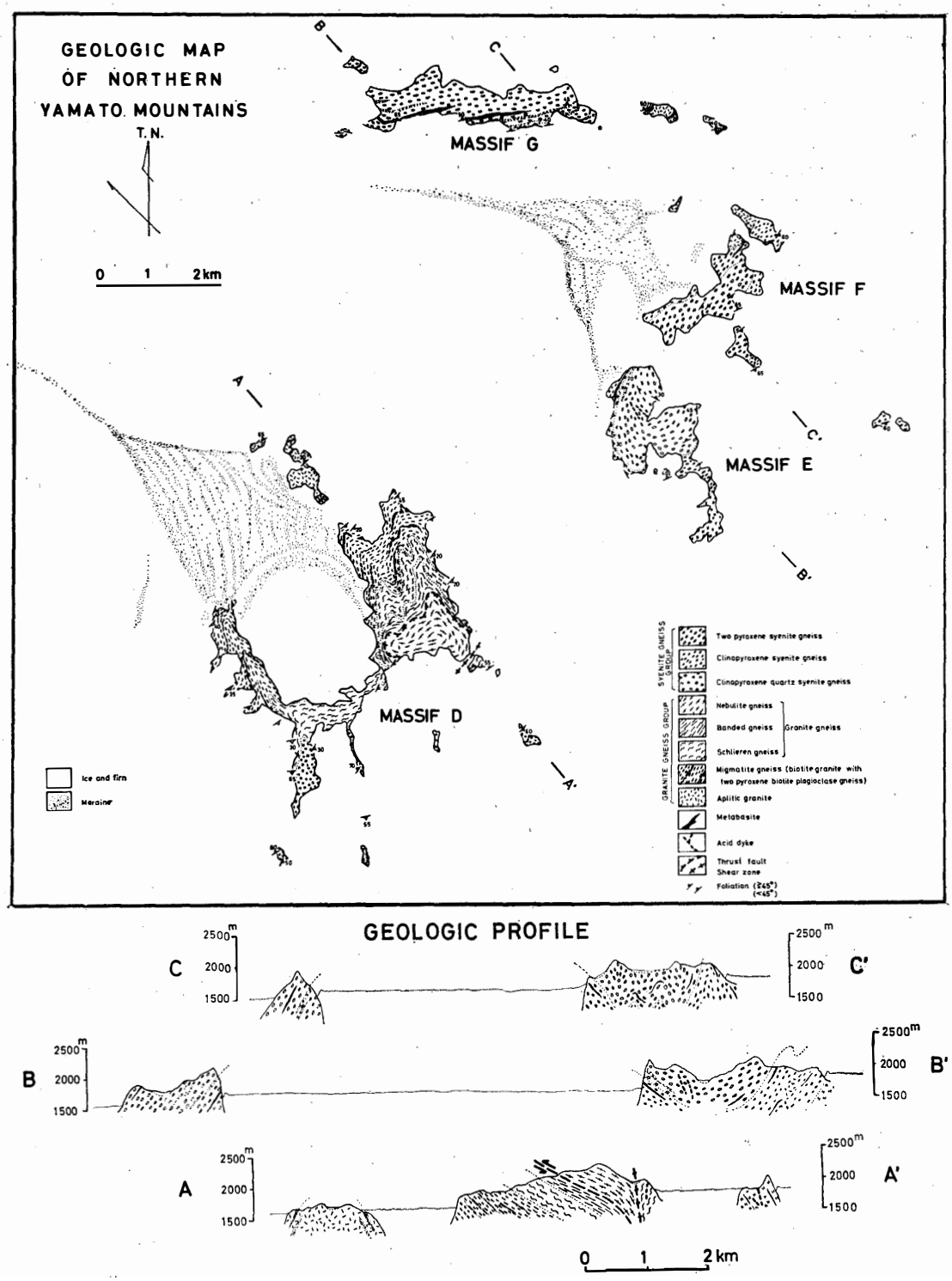

Fig. 3. Geologic map of the northern Yamato Mountains.

rarely by the parallel arrangement of potash feldspar porphyroblasts. Weathered surface of the rock is stained brownish red.

In Massif G, two-pyroxene syenite gneiss is rather different from that in the other massifs, because it frequently alternates with aplitic granite veins of 10–50 m wide. And the feature of the constituent minerals also differs from that of the other massifs as will be mentioned in Section 4.

Although the relation between the two-pyroxene syenite gneiss in Massif G and that in the other massifs is not clear due to the lack of exposure, it seems structurally that the gneiss of Massif G overlies those of Massifs E and F.

3.1.2. Clinopyroxene syenite gneiss

Clinopyroxene syenite gneiss is exposed around Massifs E and F. The rock has potash feldspar porphyroblasts as in the two-pyroxene syenite gneiss, though the porphyroblasts are light grey in colour. The rock is generally massive, while a strong foliation is occasionally observed.

The contact of the two-pyroxene syenite gneiss to the clinopyroxene syenite gneiss indicates their gradational transition, showing a schlieren structure (Fig. 15). Near the contact, paleosomes of the two-pyroxene syenite gneiss are enclosed in the clinopyroxene syenite gneiss (Fig. 16).

3.1.3. Clinopyroxene quartz syenite gneiss

Clinopyroxene quartz syenite gneiss is similar to the clinopyroxene syenite gneiss, but it contains more quartz and is more pinkish in colour. The rock is exposed at the southern end of Massif E, in the eastern part of Massif D, and in the associated nunataks. The relation between this rock and the clinopyroxene syenite gneiss is completely gradational.

3. 2. Granite gneiss group

The granite gneiss group is widely observed at Massif D and sporadically found at Massifs E, F and G and also small nunataks in the vicinity. The group corresponds to the granitic group designated by KIZAKI (1965).

From the texture of hand specimens as well as mineral composition, the granite gneiss group is classified into granite gneiss, migmatite gneiss, and associated aplitic granite.

3.2.1. Granite gneiss

Granite gneiss is subdivided into three types by the mode of occurrence. They are nebulite gneiss, schlieren gneiss and banded gneiss in terms of the definition by MEHNERT (1968), though their petrographical characters are almost identical.

Nebulite gneiss developed around the summit of Massif D shows weak foliation. The rock is medium-grained and pink in colour.

Schlieren gneiss and banded gneiss are generally fine- to medium-grained

quartzofeldspathic rocks containing abundant pink microcline (Fig. 17). Basic schlieren consisting of the aggregate of biotite and hornblende characterizes the schlieren gneiss. In the southeastern part of Massif D, the schlieren gneiss grades into the clinopyroxene quartz syenite gneiss. In the basic layer ranging from 5 to 10 m in width, the clinopyroxene quartz syenite gneiss of lenticular form and 40–60 cm in length is found as paleosomes.

Banded gneiss occurs as a narrow belt of about 100 m thick (Fig. 18). The rock consists of melanocratic layers and leucocratic ones in alternation, with a width of 2–10 mm. Mesofolding is often seen in the schlieren gneiss and the banded gneiss (Fig. 19).

3.2.2. Migmatite gneiss

Migmatite gneiss is distributed mainly in the western part of Massif D. It is conspicuous that microline grains in the rock are white in colour in contrast with those in the granite gneiss mentioned above. The rock shows a heterogeneous appearance, and consists of paleosomes of two-pyroxene biotite plagioclase gneiss and neosomes of biotite granite. Sometimes metabasite occurs as paleosome. Therefore, the rock presents agmatite, schollen, and banded structures (Figs. 20–21). Two-pyroxene biotite plagioclase gneiss which shows strong foliation is a fine-grained melanocratic rock. Biotite granite carrying purple-grey quartz grains is generally massive.

The contact between the granite gneiss and the migmatite gneiss is not clear because of many intrusions of the aplitic and pegmatitic dykes in between. However, it is noted that the foliation of the both gneisses shows the same attitude.

3.2.3. Aplitic granite

Aplitic granite occurs in a direction of NE-SW across the area surveyed. The rock occurs as a sheet-like body parallel to the foliation of the host rock (Figs. 22–23).

In hand specimens the rock is variable in feature but mostly it is a medium-grained quartzofeldspathic rock, while garnet grains are found in the central part of the body. Biotite tends to be richer at the margin. The aplitic granite intruded into the syenite gneiss has sometimes orthopyroxene relicts and is slightly brownish in colour.

3. 3. Metabasites

Metabasites are well developed throughout the whole area. There are two kinds of the metabasites. One occurs as interlayers parallel to the foliation of the host rock, and the other occurs as dykes intersecting the foliation. Metabasite interlayer, 0.2–2 m in width, shows band, lens and flame-like shapes. Most of the rocks is biotite granulite and generally has the same mineral assemblages as the host rock. The interlayer is a fine- to medium-grained foliated rock in hand specimens. In migmatite gneiss, pyroxene amphibolite interlayer occurs as paleosomes.

The rock which is about 10 m in width is agmatized by biotite granite.

Metabasite dyke is found in the northwestern part of Massif D. The rock is also agmatized by successively emplaced acid dyke.

3. 4. Acid dyke

Acid dykes which range 0.3–3 m in width occur in most parts of the area studied except Massif G. Particularly they develop in Massif D. The acid dyke is similar to pink microcline granite in composition. The grain size varies from aplite to pegmatite. The acid dykes intruded subsequently to the metabasite dyke resulting in the formation of agmatite. Consequently, the acid dyke represents the latest stage of igneous activity in the studied area.

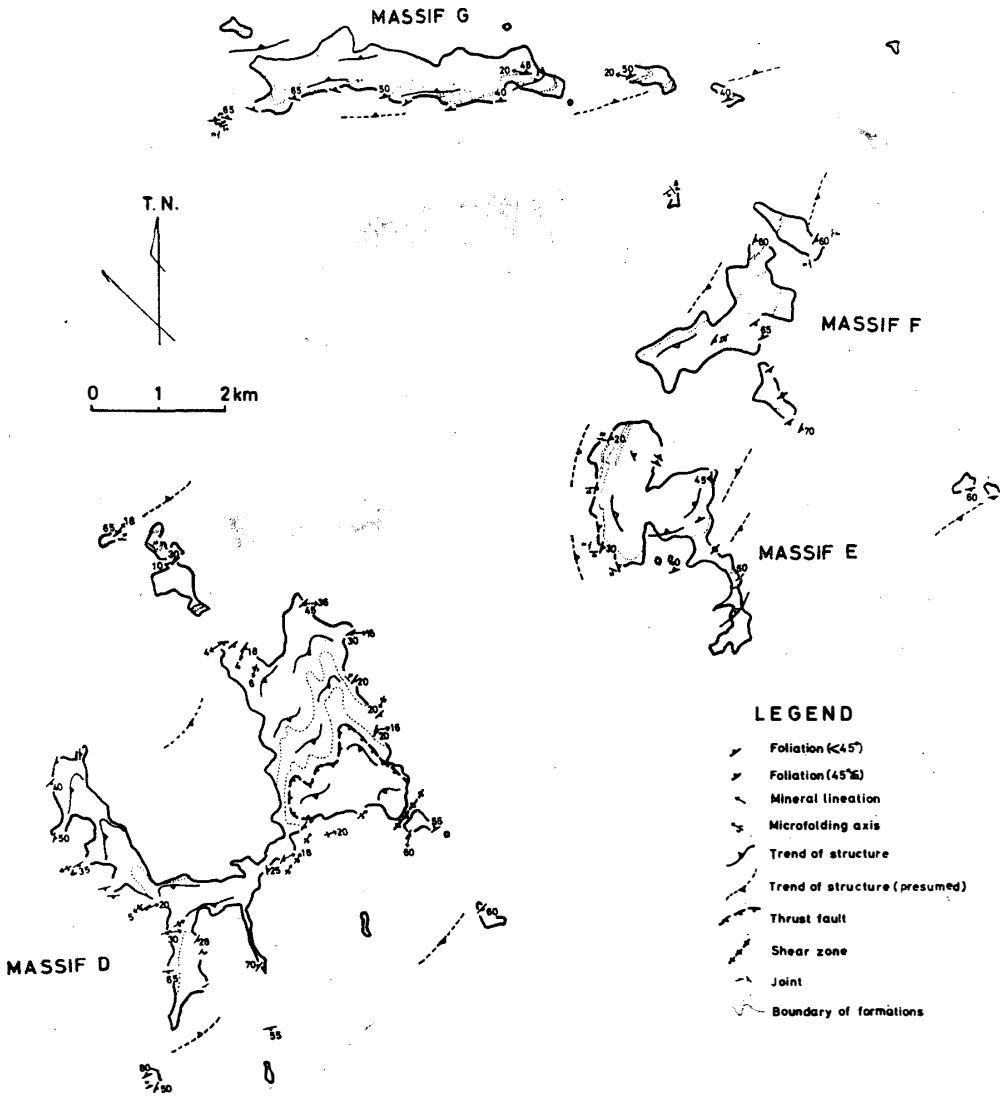

Fig. 4. Tectonic map of the northern Yamato Mountains.

3. 5. Geologic structure

The foliation in Massifs D, E and F generally trends in the NE-SW direction and dips to the east, while that in Massif G trends ENE-WSW and monoclinally dips to the north (Fig. 4). These trends of the foliation are closely correlated to the morphological arrangement of the massifs in the northern Yamato Mountains.

The foliation of Massif E shows a half basin structure open to the north. Massif D has a zone of almost vertical dip along the synclinal axis of the basin in Massif E. This corresponds to the presence of a sheared zone along the synclinal axis. Nebulite gneiss is thrust up to the west against the under-seated schlieren gneiss with almost similar dip parallel to the foliation. The foliation dips to the west at the northwesternmost nunatak of Massif D. Thus presented is an anticlinal axis of the NE-SW direction along which the aplitic granite is distributed. Mineral lineation defined by the aggregate of mafic minerals and microfolding axis develops in the granite gneiss group.

3. 6. Metamorphic history of the basement rocks

On the basis of occurrence of the rocks described above, the metamorphic history of the basement rocks is suggested as follows:

i) The two-pyroxene syenite gneiss and two-pyroxene biotite plagioclase gneiss occur usually as paleosomes and never contact with each other. Consequently, it is considered that they were derived from different original rocks of high grade metamorphism at the early stage.

ii) At the later stage, the syenite gneiss was granitized with slight mechanical disturbance.

iii) On the other hand, the two-pyroxene biotite plagioclase gneiss was migmatized and subsequently the aplitic granite intruded.

iv) The metabasite interlayers intruded before the early metamorphism, whereas the metabasite dykes intruded after the migmatization.

v) The acid dykes intruded at the latest stage.

4. Petrography

4. 1. Terminology and techniques

The structural terminology by MEHNERT (1968) related to granitic rocks and textural classifications by MOOR (1970) with modifications by COLLERSON (1974) were used in this study. Shape of grain boundary and perthitic structure were described by the same method as proposed by SPRY (1969).

Modal compositions of minerals in each thin section were calculated by counting at least 1500 points. Optical angles and plagioclase compositions were determined by means of four-axis universal stage. Refractive indices of clinopyroxenes, hornblendes, biotites and garnet, were determined by dispersion method. Unit cell dimensions of garnet, clinopyroxenes and d(060) of biotites were determined by X-ray powder diffraction patterns.

The optical properties of the constituent minerals are shown in Table 1.

4. 2. Two-pyroxene syenite gneiss

The texture is seriate amoeboid with abundant large potash feldspar porphyroblasts (Fig. 24). The following mineral assemblage is very common; potash feldspar (orthoclose)+clinopyroxene+plagioclase+biotite±hornblende+orthopyroxene+minor quartz, with accessory minerals of apatite, opaque minerals and zircon.

Potash feldspar occupies more than 50% of the constituent minerals. Most of the potash feldspar occur as porphyroblast with sutured (lobate) grain boundary. Large porphyroblast always includes many fine minerals such as opaque minerals, biotite, clinopyroxene and apatite. Ilmenite and hematite occur in liner alignment. Potash feldspar is always perthitic, and string (hair) type of mesoperthite is most common (Fig. 25). Fine-grained plagioclases with fine albite polysynthetic twinning occur around potash feldspar. In the specimen from Massif G, anti-perthitic plagioclase porphyroblasts with An 23–28 rarely are found.

Clinopyroxene occupies about 10% of the constituent minerals. It aggregates with other mafic minerals, and more or less altered into biotite and/or hornblende at margin and along cleavage. Due to abundant inclusions of apatite and opaque minerals, it often shows poikiloblastic texture. Clinopyroxene in this rock type

Table 1. Optical properties of the constituent minerals.

		1	2	3	4	5	6	7	8	9	10	11	12	13
Sample No.		208	606	3005T	605	304	303	910	907B	705	1010	1012	602	704
Plagioclase	An	23-28	n.d.	n.d.	15-28	17-24	n.d.	24-25	20-28	22-30	25-35	23-27	23	27-40
Clinopyroxene	X	colour-less	colour-less	colour-less	pl. green	pl. blu. green	lt. green	colour-less			colour-less		colour-less	colour-less
	Y	〃	〃	〃	lt. green	pl. green	pl. green	〃			〃		〃	〃
	Z	〃	〃	〃	pl. green	〃	yel. green	〃			〃		〃	〃
	α	1.698	1.693	n.d.	1.701	1.697	1.699	n.d.			n.d.		n.d.	n.d.
	γ	1.724	1.715	1.725	1.726	1.719	1.723	1.720			1.715		1.714	1.728
	$2V_z$	53-58	60.5	42-64	53-58	49-69	53	50-64			53-58		46-56	58-50
	cz	42	42	41	41.5	44-47	n.d.	47-49			40		41	40-45
Orthopyroxene	X	colour-less	colour-less	colour-less							colour-less		colour-less	
	Y	〃	〃	〃							〃		〃	
	Z	〃	〃	〃							〃		〃	
	$2V_z$	59	47-54	50							43-58		40-58	
Hornblende	X	lt. brown		lt. yel. brown	pl. yellow	yel. brown	pl. grn. yellow	pl. green	dk. brn. green	pl. grn. brown				pl. brown
	Y	brown		lt. grn. brown	brn. brown	brn. green	pl. green	brn. green	lt. grn. yellow	pl. brown				brn. green
	Z	brown		dk. brn.	lt. yel.	green	blu. green	dk. green	dk. green	brn. green				green
	α	1.658		n.d.	n.d.	1.664	n.d.	1.668	n.d.	n.d.				n.d.
	γ	1.683		1.685	1.670	1.675	1.676	1.687	1.699	1.699		Garnet		1.678
	$2V_x$	77-83		70-85	81-83	67-79	51-67	56-70	30-50	65-74		γ=1.795		78-84
	cz	20-31		20	16	19	18	n.d.	n.d.	11		a=11.543 (Å)		10-24
Biotite	Z′	red. brown	red. brown	red. brown		yel. brown	dk. brown	brown	dk. brown	red. brown	red. brown	dk. brown	brown	brown
	γ	1.636	1.640	1.641		1.629	1.637	1.653	1.655	1.657	1.642	1.646	1.624	1.623

1, 2, 3: Two-pyroxene syenite gneiss.

4, 5: Clinopyroxene syenite gneiss.

6, 7: Clinopyroxene quartz syenite gneiss.

8: Granite gneiss.

9: Biotite granite.

10: Two-pyroxene biotite plagioclase gneiss.

11: Aplitic granite.

12: Pyroxene granulite.

13: Pyroxene amphibolite.

lt.=light
dk.=dark
pl.=pale
brn.=brownish
grn.=greenish
blu.=bluish
yel.=yellowish

shows no pleochroism and is colourless or very pale green. Orthopyroxene is a characteristic mineral of this rock type, though it always occurs only as relict mineral with clinopyroxene. It shows no pleochroism and is colourless. Biotite is relatively fresh and contains less inclusions. It occurs closely associated with clinopyroxene. Hornblende is often poikiloblastic with inclusions of quartz, apatite and clinopyroxene. It is noteworthy that the hornblende of Massif G is brown in colour, while that of Massifs E and F is greenish. Xenoblastic quartz grains rarely occur as fine round grains scattered around mafic aggregates.

4. 3. Clinopyroxene syenite gneiss

The texture of this rock is generally inequigranular interlobate, although it tends to be seriate and amoeboid. This rock carries abundant large porphyroblasts of light grey potash feldspar. The mineral assemblage is potash feldspar+biotite± hornblende+clinopyroxene+plagioclase+quartz, with apatite, opaque minerals, sphene and zircon.

The potash feldspar is also main constituent mineral over 50% in volume. The grain size usually ranges from 0.8 cm to 3.0 cm, and sometimes attains 6 cm in maximum. It has perthitic structure of ribbon or flame type (Fig. 26). Albite occurring as perthite lamellae shows polysynthetic twins. On the other hand, potash feldspar has albitic rims as described by RAMBERG (1962). The albite rim is connected with perthite lamellae having the same extinction position. Sometimes hair perthite occurs with the broad perthite mentioned above, but differs in orientation from the latter (Fig. 27). Potash feldspar generally shows undulatory extinction and rarely exhibits microcline grid in a limited part of some grains. Inclusions which are apatite, clinopyroxene, biotite and opaque minerals in the porphyroblast of potash feldspar are less than in those of two-pyroxene syenite gneiss. Pigments of opaque minerals such as observed in the two-pyroxene syenite gneiss are rare. Plagioclase occurs as perthite lamellae and rim around potash feldspar grains. Therefore, its amount depends on the development of perthite lamellae and plagioclase rims, and varies from 5% to 27% in the constituent minerals.

Clinopyroxene is common and occupies up to 10% of the constituent minerals, and frequently altered to hornblende or biotite (Fig. 28). It occurs as poikiloblastic crystals. It is pale greenish in colour and shows weak pleochroism. Biotite and hornblende generally occur with clinopyroxene and often as inclusions in clinopyroxene. Biotite itself has inclusions of apatite, opaque minerals, quartz and zircon. Quartz grains which often show strong undulatory extinction have rounded form and are mainly associated with mafic minerals.

4. 4. Clinopyroxene quartz syenite gneiss

The texture is variable and complicated but generally shows seriate amoeboid (Fig. 29). Potash feldspar porphyroblasts develop widely throughout the area.

Mineral assemblage of the clinopyroxene quartz syenite gneiss is rather uniform and similar to that of the clinopyroxene syenite gneiss. However, the properties of each mineral are somewhat different from the latter. The following assemblage is common: potash feldspar+plagioclase+quartz+hornblende+biotite+clinopyroxene (relic)+sphene+apatite+opaque minerals+zircon.

Potash feldspar is a main constituent mineral (about 50% in volume). The grain size varies from 0.8 cm to 3.0 cm. Generally the grain boundary is well sutured, and filled up with albite (–oligoclase). Perthites are well developed, showing ribbon, flame (plume), braid and patch type in shape (Figs. 30–31). Potash feldspar may be intermediate closer to maximum microcline because the grid is sharp near the perthite lamellae. Sometimes, potash feldspar is completely disintegrated by plagioclase, and shows ganglia-like structure (AUGUSTITHIS, 1973). Independent grains of plagioclase are limited in amount, and they seem to have been derived from perthite lamellae. They are enveloped by perthitic potash feldspars and quartz. Myrmekitic texture is often found.

Xenoblastic quartz grains with curved to embayed boundaries make up 1–15% of the rock. Most grains show undulatory extinction and have very fine inclusions like bubbles which show occasionally linear arrangements. Hornblende is generally poikiloblastic and rounded. They are frequently altered to biotite. The grain size varies from 0.2 mm (rounded grain) to 2.0 mm (poikiloblast). It is conspicuous that the pleochroism Z is bluish green. Biotite poikiloblasts including opaque minerals are observed, especially along the cleavage. Clinopyroxene shows rather strong pleochroism of bluish green. It occurs as relict mineral (0.1–2.0 mm), and generally makes up a few percent of the rock. Occasionally it is almost completely altered to hornblende or biotite. Sphene is an abundant accessory mineral, up to 1% in volume. Generally it fringes opaque minerals and is associated with mafic minerals. The grain size reaches 2 mm in length (Fig. 32). Opaque minerals make up over 2% of the rock in maximum.

4. 5. Granite gneiss

Nebulite gneiss and schlieren gneiss show similar textures under the microscope, *i.e.* inequigranular interlobate to amoeboid, though the former includes melanosome which is equigranular. The texture of banded gneiss is granoblastic but slightly elongated due to the presence of elongated quartz grains (Fig. 33).

Mineral assemblage of granite gneiss is uniform and consists essentially of potash feldspar (microcline)+quartz+plagioclase (oligoclase)+biotite with or without hornblende. Accessories are apatite, opaque minerals, zircon and sphene. Potash feldspars make up about 40% of the rock. Most of them are perthite of stringlet type (Fig. 34). They are microcline showing distinct grid texture. Quartz grains in the banded gneiss and occasionally in the nebulite gneiss are elongated up to 4.0 mm in length. Such grains are cracked and show strong undulatory extinction. Plagioclase is characterized by albite twinning and myrmekitic texture.

Biotite is the main mafic mineral. Biotite laths show preferred orientation with hornblende laths particularly in the banded gneiss. Hornblende and biotite are often altered to chlorite.

4. 6. Migmatite gneiss

Migmatite gneiss consists of biotite granite and two-pyroxene biotite plagioclase gneiss which are the neosome and paleosome, respectively.

4.6.1. Biotite granite

Texture is inequigranular interlobate to amoeboid (Fig. 35). Mineral assemblage is as follows: potash feldspar (microcline) +quartz+plagioclase+hornblende+biotite+apatite+opaque minerals+sphene+zircon. Sericite and chlorite are secondary products of feldspars, biotite and hornblende.

Potash feldspar, ranging from 0.5 to 7.0 mm in size, constitutes about 50% of the rock. The grains are almost perthitic of stringlet shape, and show grid texture of undulatory extinction. Potash feldspar in hand specimens is white in colour. Hornblende and biotite are similar in amount. Conversion from hornblende to biotite is often observed. Biotite lath includes rounded quartz grains.

4.6.2. Two-pyroxene biotite plagioclase gneiss

The texture is equigranular to inequigranular of interlobate. The following mineral assemblages are found:

i) plagioclase+quartz+potash feldspar+biotite+hornblende+clinopyroxene ±orthopyroxene

ii) plagioclase+quartz+biotite±clinopyroxene

The first mineral assemblage is found in paleosome in migmatite gneiss, whereas the second in the western part of Massif D, where aplitic granite intrudes. Other minerals are apatite, opaque minerals and zircon.

Plagioclase is the most common mineral, being 0.3–2.0 mm in size. Albite and pericline twins are common. The grains are often deformed and kinking of the twinned lamellae is observed. The An content of plagioclase in assemblage ii) is rather higher than that in assemblages i). Biotite laths have a strong preferred orientation, giving an intense schistosity to the rock. Some biotites show "myrmekite-like" texture along the cleavage due to intergrowth with quartz grains. Pleochroism of clinopyroxene is very weak, colourless to pale green. It is partly altered to biotite and hornblende. Orthopyroxene is rarely found but is almost converted to clinopyroxene (Fig. 36). Potash feldspar rarely occurs. It is perthitic with stringlet type, but never shows microcline grid. Some show undulatory extinction. Hornblende is dominant in assemblage i). It shows characteristic pleochroism, Z–dark green. Biotite is more predominant than hornblende in many cases.

4. 7. Aplitic granite

Mineral assemblage of the rock is as follows: Potash feldspar+quartz+plagioclase±biotie±garnet. Very small amounts of opaque minerals, zircon, muscovite are observed as accessory minerals.

Potash feldspar, 0.5–4.0 mm, is always larger in amount than plagioclase. Most of the potash feldspar show microcline grid and are perthitic of stringlet type. Graphic intergrowth of quartz and potash feldspar is common. Garnet is not abundant but characteristic mineral of the rock. The garnet grains, 0.8–5.0 mm in size, show slightly idiomorphic form though they usually have cracks. The crack is filled up with muscovite and biotite. It is pale pinkish in colour.

4. 8. Metabasite

Metabasite interlayers can be divided into two types as follows:

i) biotite granulite: potash feldspar+biotite+clinopyroxene+orthopyroxene±quartz.

ii) pyroxene amphibolite: plagioclase+hornblende+clinopyroxene+biotite ±orthopyroxene.

4.8.1. Biotite granulite

The texture of biotite granulite is generally equigranular interlobate to slightly polygonal, although some potash feldspars are porphyroblastic (Fig. 37). Potash feldspar is perthitic, belonging to fine hair type and occasionally shows undulatory extinction. Some grains have Carlsbad twins. When small quartz grains are in contact with potash feldspar, micrographic texture is formed. Accessories are apatite, opaque minerals and zircon. Apatite attains up to 3% of the rock.

4.8.2. Pyroxene amphibolite

The texture of amphibolite is equigranular polygonal. Biotite and hornblende are aligned in a preferred orientation (Fig. 38). Plagioclase shows albite, pericline and their composite twins. The An content of the plagioclase is up to 40%. Hornblende encloses clinopyroxene and plagioclase. Some poikiloblastic clinopyroxene grains are often converted to hornblende. Orthopyroxene is found as small rounded grain, although it is less in amount.

4. 9. Acid dyke

The grain size is variable from fine to coarse. The mineral assemblage is as follows: potash feldspar+quartz+plagioclase+biotite±hornblende.

Potash feldspar is the most abundant and shows microcline grid. It has amoeba-like quartz as inclusions, showing graphic texture. Quartz shows always undulatory extinction. Mafic minerals are rare, only a few percent in volume.

4. 10. Metamorphic grade

The two-pyroxene syenite gneiss contains orthopyroxene as relict mineral and

orthoclase. Orthopyroxene is a diagnostic mineral of the granulite facies. On the other hand, the granite gneiss contains microcline perthite and never contains orthopyroxene. This fact suggests that the granite gneiss belongs to the amphibolite facies (MIYASHIRO, 1973).

Orthopyroxene is also observed in the two-pyroxene biotite plagioclase gneiss which occurs as paleosomes in the migmatite gneiss. This rock type has the same mineral assemblage as that of the two-pyroxene syenite gneiss.

The marked difference of the mineral assemblages as mentioned above and the geological observations suggest that the rocks of the granulite facies suffered the later metamorphism of the amphibolite facies conditions in this area. Consequently the transition from the granulite facies to the amphibolite facies is a reflection of "activation" in the present area.

5. Gradational Relation from Syenite Gneiss to Granite Gneiss

As suggested from the field occurrences, it is clear that a gradational conversion from syenite gneiss to granite gneiss took place. Fig. 5 shows the Q-Pl-Kf plots of modal analyses of 35 rocks from the present area. They fall in separate areas in the diagram. The gradational sequence from the two-pyroxene syenite gneiss to the clinopyroxene quartz syenite gneiss is characterized by the decrease of potash feldspar, and that from the clinopyroxene quartz syenite gneiss to granite gneiss by the increase of quartz and the slight decrease of potash feldspar.

5. 1. Texture and mineral assemblage

Textures shown in the series can be divided into the following two types:

i) seriate amoeboid to inequigranular interlobate in syenite gneiss.

ii) inequigranular amoeboid to equigranular interlobate in granite gneiss.

The difference between i) and ii) is also reflected on their grain size. The former mostly contains large potash feldspar porphyroblasts and consists of coarse-grained minerals, whereas the latter is composed of medium grained minerals

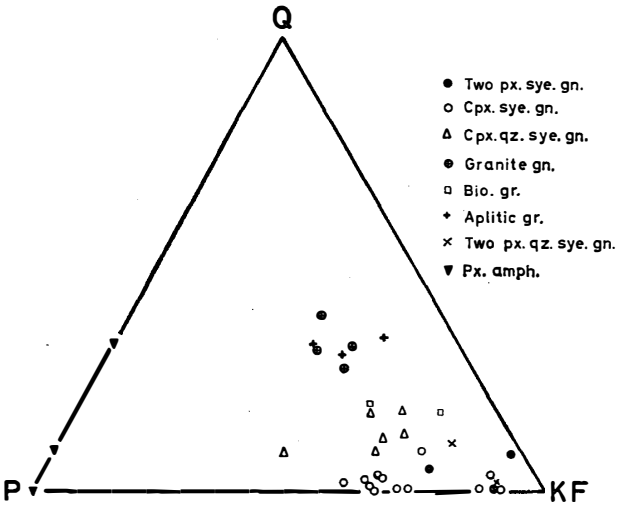

Fig. 5. Modal relationship in Q-Pl-Kf diagram.

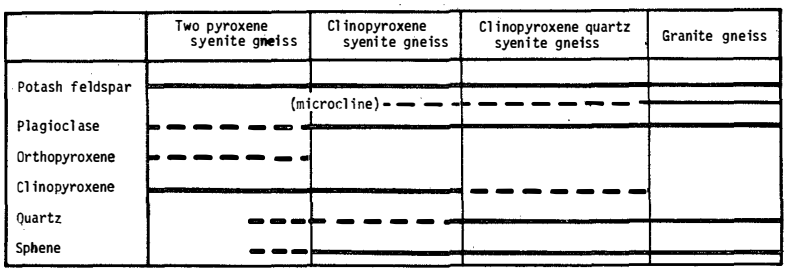

Fig. 6. Change of mineral assemblage with respect to the granitization.

although potash feldspar porphyroblasts occasionally occur.

From the evidences mentioned in Section 4, the changes of mineral assemblages with respect to the gradation from the two-pyroxene syenite gneiss to the granite gneiss are shown in Fig. 6.

5. 2. Perthite

Potash feldspar is the most dominant constituent mineral. The mineral is always perthitic with various shapes. The characteristic perthite of each rock type can be summarized as follows:

i) stringlet (hair) in the two-pyroxene syenite gneiss,

ii) ribbon, flame and braid in the clinopyroxene syenite gneiss and the clinopyroxene quartz syenite gneiss,

iii) stringlet (drop) in the granite gneiss.

This classification is not rigid and is made by using the most dominant type of feldspars.

The hair perthite has fine albite lamellae and is mesoperthitic. Occasionally a part of the perthite grain shows undulatory extinction, indicating that this mineral is cryptoperthite.

In the clinopyroxene syenite gneiss the hair perthite is obliquely cut by the flame perthite (Fig. 27). On the other hand, albite rim is observed along the grain boundary of the potash feldspar and the flame perthite lamellae seems to be connected with the rim (Fig. 31). Consequently, the above observations suggest that the hair perthite was formed by the different mechanism and at the different stage from the other perthite.

5. 3. Hornblende and biotite

Fig. 7 shows relationships of refractive indices (γ) between hornblende and biotite. There is a positive correlation between them. It seems that each rock type occupies the determined compositional field although they are overlapped. From the viewpoint of the gradational sequence of the rocks, the refractive index of each

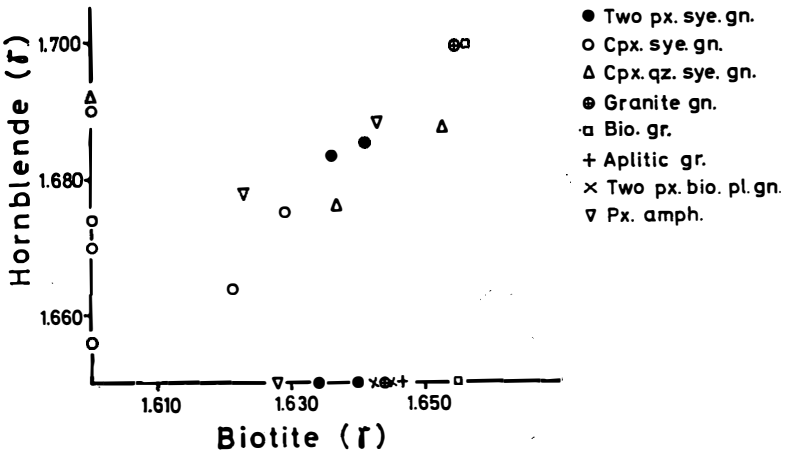

Fig. 7. Relation between the refractive index (γ) of biotite and coexisting hornblende. The refractive index of the both minerals which are not associated with each other is shown on the abscissa or ordinate.

mineral decreases from the two-pyroxene syenite gneiss to the clinopyroxene syenite gneiss and then increases to the granite gneiss.

5. 4. Fe/(Fe+Mg) ratio of biotite

Measurement of d(060) value with X-ray diffractometer was carried out on 15 selected biotites (WONES, 1963; PEIKERT, 1963). Four of 15 are from the rock types which do not belong to the gradational sequence. Each peak has rela-

Table 2. D(060) spacing and refractive index (γ) of biotite.

Sp. no.	d(060) (Å)	R.I. (γ)	
209A	1.5415	1.636	Two-pyroxene syenite gneiss
3005T	1.5399	1.641	"
606	1.5379	1.640	"
904B	1.5379	1.621	Clinopyroxene syenite gneiss
304	1.5390	1.629	"
402	1.5404	—	"
601	1.5386	—	"
303	1.5418	1.637	Clinopyroxene quartz syenite gneiss
910	1.5408	1.653	"
907B	1.5437	1.655	Granite gneiss
713	1.5415	1.644	"
712	1.5414	1.657	Biotite granite
1012	1.5428	1.646	Aplitic granite
1010	1.5419	1.642	Two-pyroxene biotite plagiclase gneiss
704	1.5405	1.623	Pyroxene amphibolite

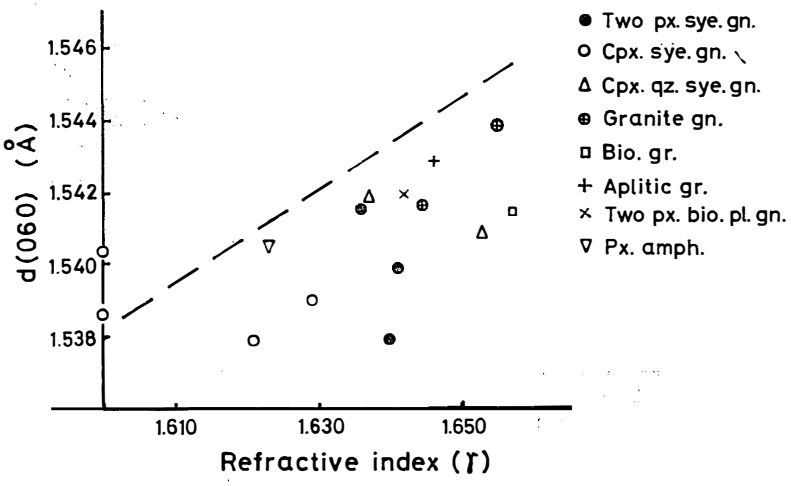

Fig. 8. Relationship between the refractive index (γ) and d(060) spacing of biotite.

tively low intensity because of the preferred orientation of the biotite. The values are shown in Table 2. In Fig. 8, d(060) values are plotted against refractive index, although this relationship becomes obscure in the two-pyroxene syenite gneiss. Broken line shows synthetic biotite on the join phlogopite-annite. The refractive indices of the biotite in this area are higher than those of synthetic biotites. The biotite in the two-pyroxene syenite gneiss is not plotted on the general trend.

This phenomenon leads to the following consideration. The Ti content in biotite also increases with the increase of the refractive index (ENGEL and ENGEL, 1960; DEER *et al.*, 1963). The two-pyroxene syenite gneiss has less amount of sphene, but in the clinopyroxene syenite gneiss, especially clinopyroxene quartz syenite gneiss, sphene frequently occurs with biotite and opaque minerals (Fig. 32). Therefore, the biotite of the two-pyroxene syenite gneiss is considered to be higher in the Ti content than the other syenite gneisses. Colour of each biotite seems to support the explanation. Biotite in the two-pyroxene syenite gneiss is reddish brown showing higher Ti content, while that in the other syenite gneisses is yellowish brown to brown showing lower Ti content (see 5.6.).

5. 5. Clinopyroxene

Refractive indices of clinopyroxenes seem to show no systematic relation among rock types. Until-cell parameters were measured for five samples (Table 3). The data were plotted in the diagram after BROWN (1960) (Fig. 9). In the figure they fall in almost the same area, though the clinopyroxene quartz syenite gneiss is rather rich in Fe.

The compositions estimated from the unit-cell ($a \sin \beta$) and the refractive index (γ) were plotted in the diagram of NOLAN (1969) (Fig. 10). The figure

Table 3. Unit-cell parameters of clinopyroxene.

	a (Å)	b (Å)	c (Å)	β (deg.)	V (Å^3)
1	9.755 ±0.002	8.933 ±0.001	5.249 ±0.003	105.80 ±0.02	440.1 ±0.2
2	9.757 ±0.001	8.933 ±0.001	5.253 ±0.002	105.98 ±0.01	440.2 ±0.2
3	9.754 ±0.006	8.932 ±0.001	5.228 ±0.012	105.90 ±0.05	438.0 ±1.0
4	9.751 ±0.003	8.928 ±0.001	5.247 ±0.004	105.95 ±0.03	439.2 ±0.4
5	9.762 ±0.003	8.950 ±0.001	5.240 ±0.001	105.79 ±0.05	440.5 ±0.2

1. Two-pyroxene syenite gneiss from Massif G (209A)
2. Two-pyroxene syenite gneiss from Massif F (606)
3. Clinopyroxene syenite gneiss from Massif F (605)
4. Clinopyroxene syenite gneiss from Massif E (304)
5. Clinopyroxene quartz syenite gneiss from Astronomical point (303)

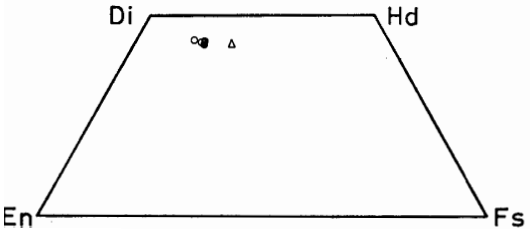

Fig. 9. Compositions of clinopyroxene after BROWN'S *diagram. Symbols are in same as in Fig. 8.*

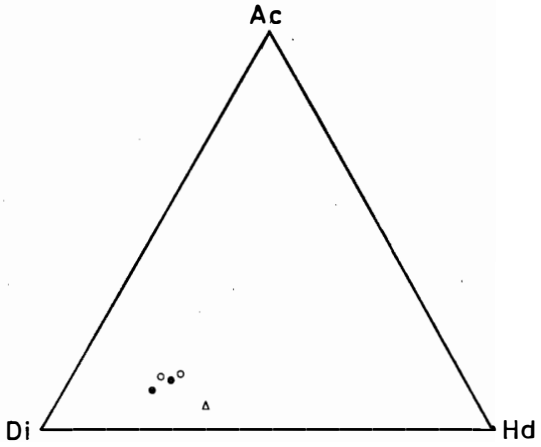

Fig. 10. Compositions of the clinopyroxene after NOLAN'S *diagram. Symbols are the same as in Fig. 8.*

shows that the acmite molecule tends to increase from the two-pyroxene syenite gneiss to the clinopyroxene syenite gneiss and then hedenbergite molecule increases. As will be mentioned in Section 6, the rocks in this area are rather rich in Fe^{3+} and Na. The oxidation ratio in the bulk compositions of the rocks culminates in the clinopyroxene quartz syenite gneiss. The culmination of the oxidation of the clinopyroxene does not seem to coincide with that observed in the bulk composition.

5. 6. Colour of biotite and hornblende

Throughout the whole area it is noteworthy that the axial colour of minerals such as biotite and hornblende seems to depend upon the rock type (Table 1). The change in colour of biotite from the two-pyroxene syenite gneiss to the clinopyroxene syenite gneiss seems to be due to the decrease of the TiO_2 content and the increase of $Fe_2O_3/(Fe_2O_3+FeO)$, and the change from the clinopyroxene syenite gneiss to the granite gneiss is mainly due to the decrease of $Fe_2O_3/(Fe_2O_3+FeO)$ ratio (HAYAMA, 1959; ENGEL and ENGEL, 1960).

For hornblende it is conspicuous that the hornblende from Massif G which is brownish in contrast with that from the Massifs E and F. The difference between them seems to be due to the content of TiO_2 (BINNS, 1965; LEAKE, 1965).

5. 7. Summary

The gradational sequence from the two-pyroxene syenite gneiss to the granite gneiss is probably reflecting not only the textural features and mineral assemblages but also the presumed chemical compositions of the constituent minerals. They are summarized as follows:

i) The hair type of perthite is dominant in the two-pyroxene syenite gneiss and successively the flame, ribbon and blade types are developed at the later process.

ii) The Fe/Fe+Mg ratio of biotite increases towards the granite gneiss, and that of hornblende and clinopyroxene may also increase with that of biotite.

iii) The Ti content of biotite is richer in the two-pyroxene syenite gneiss.

These phenomena may indicate that the two-pyroxene syenite gneiss which was formed under the granulite facies conditions was activated under the amphibolite facies conditions resulting in the granite gneiss.

6. Petrochemistry

Major elements of twelve rocks were analyzed by the wet chemical method. Eleven of them are selected along the gradational sequence and one is from biotite granite. In addition to them, analyses of six samples from the present area and the southern Yamato Mountains by KIZAKI (1965) were used for discussion. The chemistry of major elements and C.I.P.W. norm are listed in Table 4.

6. 1. NIGGLI plots and origin of the pyroxene syenite gneiss

As mentioned in Section 3, two different rock types are distributed in the surveyed area, one became the pyroxene syenite gneisses and the other became the biotite plagioclase gneiss occurring as paleosomes in the migmatite gneiss. The pyroxene syenite gneiss, though it represents more or less the effect of granitization, preserves the granulite facies features.

Following the procedure outlined by BARTH (1966), NIGGLI numbers were calculated for the pyroxene syenite gneisses of the northern Yamato Mountains and were compared with the metabasites of the southern Yamato Mountains. They were plotted on the diagrams by the methods of SIMONEN (1953), EVANS and LEAKE (1960) and LEAKE (1964).

All these plots show that the pyroxene syenite gneisses may have been derived from igneous rocks rather than sedimentary rocks. In Fig. 11a, they fall in the volcanogeneous field but they are also included in the calcareous sedimentary field. In Fig. 11b, three pyroxene syenite gneisses are located not in the sedimentary field but in the igneous field. In Fig. 11c, they fall near by Karroo dolerite trend and not in the pelite-limestone mixture field.

From these three figures, the two-pyroxene syenite gneiss seems to have been derived from igneous rocks. The original igneous rocks, however, were not always igneous body, since pyroclastic sediments also have the igneous nature in chemical composition.

The open circles in the figures show metabasite layers and dykes from Massifs B and C. NIGGLI number of them fall near the pyroxene syentie gneiss, but subsequent amphibolite dyke falls rather far from the pyroxene syenite gneiss field in Fig. 11a.

Table 4. Chemical compositions.

	1	2	3	4	5	6	7	8	9	10	11	12
Sp. no.	606	802	304	601	402	510	406	303	904A	905	715	705
SiO_2	55.58	56.60	57.69	58.08	58.09	58.75	61.64	63.33	63.80	64.25	70.53	64.58
TiO_2	0.71	0.80	0.80	1.00	0.76	0.96	0.77	0.74	0.59	1.00	0.34	0.71
Al_2O_3	14.44	14.19	14.18	15.38	15.67	15.26	14.72	14.46	15.87	15.05	14.94	15.48
Fe_2O_3	1.29	1.51	3.13	1.85	1.99	2.23	2.66	1.43	2.08	2.25	0.65	1.60
FeO	4.32	3.73	3.02	3.21	3.64	3.06	2.89	2.63	1.41	2.14	1.42	2.79
MnO	0.06	0.08	0.06	0.04	0.06	0.05	0.03	0.03	0.03	0.04	0.02	0.03
MgO	5.55	5.40	3.47	3.39	3.50	2.85	1.99	2.59	0.96	1.14	0.73	0.75
CaO	5.85	5.65	4.69	4.65	4.42	3.93	2.81	3.10	2.25	1.94	1.48	2.49
Na_2O	3.76	3.65	3.78	3.98	3.70	4.40	4.36	3.56	4.16	4.28	3.62	3.22
K_2O	5.83	6.54	7.62	7.23	6.87	7.36	7.04	6.94	7.29	6.74	5.74	7.00
P_2O_5	0.81	0.85	0.76	0.72	0.58	0.57	0.35	0.56	0.21	0.35	0.13	0.26
$H_2O(+)$	0.55	0.44	0.40	0.36	0.56	0.22	0.35	0.24	0.19	0.38	0.30	0.36
$H_2O(-)$	0.41	0.32	0.20	0.40	0.20	0.34	0.33	0.18	0.27	0.10	0.18	0.16
Total	99.16	99.76	99.80	100.29	100.04	99.98	99.94	99.79	99.11	99.66	100.08	99.43
*	35.9	35.0	48.8	44.9	46.8	50.2	60.0	46.1	65.9	67.4	60.9	76.1
**	0.51	0.54	0.57	0.54	0.55	0.52	0.52	0.56	0.54	0.51	0.51	0.59
***	21.05	25.71	48.78	34.78	32.00	39.44	45.95	32.73	56.52	48.23	28.57	33.90

C.I.P.W. norm

Q		—	—	—	—	—	—	3.06	7.93	7.51	9.61	23.42	13.03
or		34.50	38.40	45.08	42.85	40.62	43.41	41.74	41.18	42.85	40.07	33.95	41.18
ab		26.74	26.21	25.69	28.84	31.46	30.93	36.70	29.88	35.13	36.18	30.41	27.26
an		5.28	3.06	1.39	2.78	5.84	0.28	—	3.06	3.34	1.95	6.40	7.23
ne		2.84	2.56	2.56	2.56	—	3.41	—	—	—	—	—	—
ol	fo	6.26	5.49	6.51	2.74	3.66	1.83	—	—	—	—	(c)0.51	—
	fa	2.85	2.04	2.11	1.02	1.83	0.71	—	—	—	—	—	—
hy	en	—	—	(ac)1.39	—	0.20	—	1.51	4.02	—	1.20	—	1.41
	fs	—	—	—	—	—	—	0.53	1.58	—	0.26	—	1.85
	wo	7.55	8.13	7.78	6.50	5.23	6.50	4.99	3.60	2.90	2.09	—	1.28
di	en	4.92	5.62	5.62	4.52	3.31	4.52	3.41	2.41	2.41	1.61	0.93	0.50
	fs	2.11	1.85	1.45	1.45	1.38	1.45	1.19	0.92	—	0.26	1.81	0.79
mt		1.85	2.08	3.94	2.78	2.78	3.24	3.94	2.08	3.01	3.24	0.51	2.32
il		1.37	1.52	1.52	1.97	1.52	1.82	1.52	1.37	1.06	1.97	0.61	1.37
ap		2.02	2.02	1.68	1.68	1.35	1.35	0.67	1.35	0.34	0.67	0.34	0.67
Total		98.29	98.98	99.33	99.69	99.38	99.45	99.26	99.38	98.55	99.11	99.96	98.89

1, 2: Two-pyroxene syenite gneiss
3, 4, 5, 6: Clinopyroxene syenite gneiss
7, 8, 9, 10: Clinopyroxene quartz syenite gneiss
11: Granite gneiss
12: Biotite granite

Analyst: K. SHIRAISHI

* $\frac{(2Fe_2O_3+FeO)\times 100}{2Fe_2O_3+FeO+MgO}$ mol.

** $\frac{K_2O}{Na_2O+K_2O}$ mol.

*** $\frac{2Fe_2O_3\times 100}{2Fe_2O_3+FeO}$ mol.

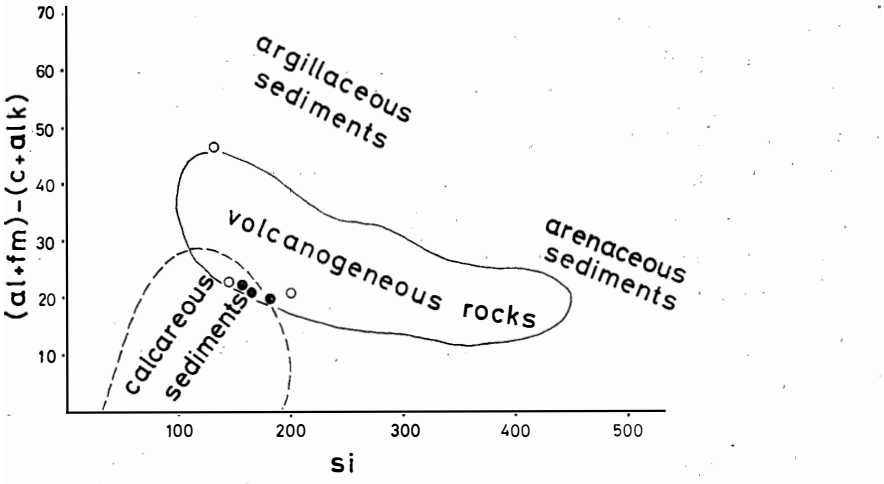

Fig. 11a. The NIGGLI *value* (al+fm)−(c+alk) *versus* si *for two-pyroxene syenite gneiss (solid circle) and metabasite (open circle) after* SIMONEN *(1953).*

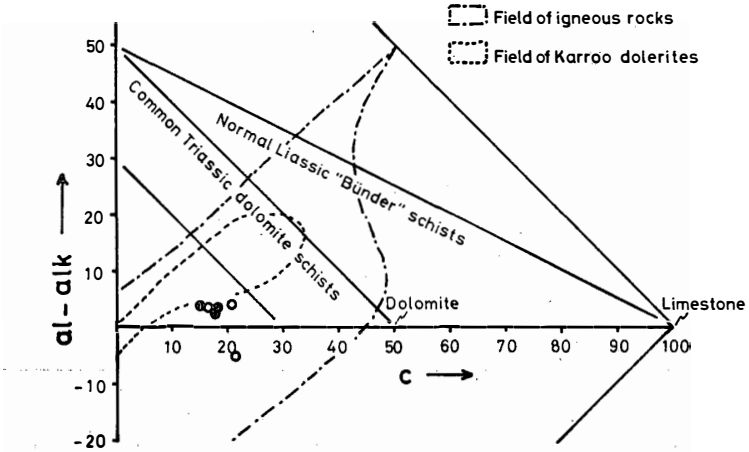

Fig. 11b. The NIGGLI *value* al-alk *against* c *after* EVANS *and* LEAKE *(1960). Symbols are the same as in Fig. 11a.*

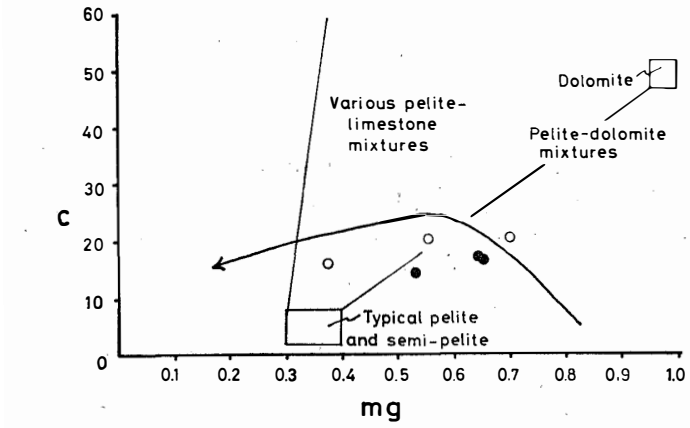

Fig. 11c. The NIGGLI *value* c *against* mg. *The trend line for Karroo dolerites is marked (*LEAKE, *1964). Symbols are the same as in Fig. 11a.*

6. 2. Chemical behaviours with respect to grantization

In the section of field geology, it was pointed out that the pyroxene syenite gneisses was transformed to the granite gneiss via the quartz syenite gneiss. This process is a key to the later metamorphism (subsequent amphibolite facies metamorphism, *i.e.* activation) in the present area.

6.2.1. Oxides–SiO_2 variation diagram

In Fig. 12, each oxide is plotted against SiO_2. As mentioned in Section 5, the granitization in the present area signifies essentially the addition of silica. Therefore, the increase of SiO_2 roughly indicates progress of the granitization process.

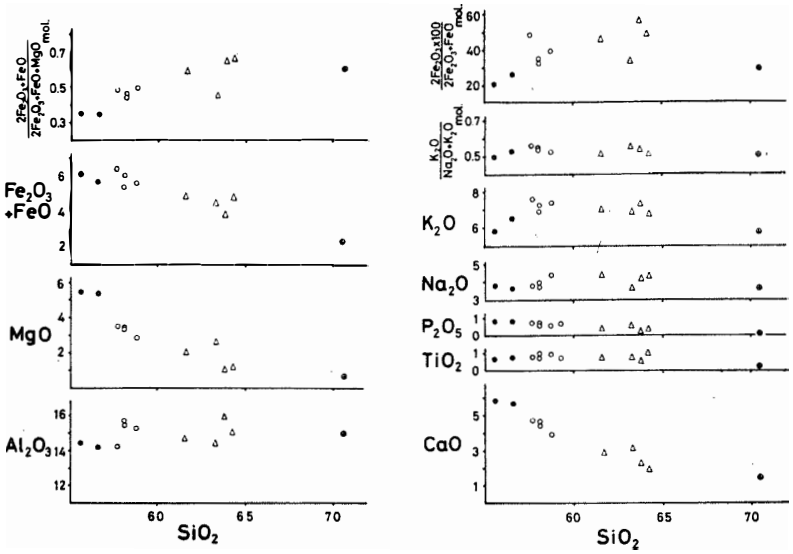

Fig. 12. Oxide variation diagram versus SiO_2. Mol ratio of ferromagnesian and alkali oxides are also shown. Symbols are the same as in Fig. 8.

i) CaO, MgO and total Fe decrease with the increase of SiO_2. This change is explained by the decrease of mafic minerals with the progress of the granitization.

ii) Na_2O and K_2O also tend to decrease.

iii) The $(Fe_2O_3+FeO)/(Fe_2O_3+FeO+MgO)$ ratio increases towards the clinopyroxene quartz syenite gneiss and decreases towards the granite gneiss.

iv) The oxidation ratio [mol. $(2Fe_2O_3\times100)/(2Fe_2O_3+FeO)$] calculated by the method of CHINNER (1960) also increases towards the clinopyroxene quartz syenite gneiss and decreases towards the granite gneiss.

6.2.2. Normative q-or-ab-ne diagram

Normative "q", "or", "ab", and "ne" are plotted in Fig. 13. Most of the two-pyroxene syenite gneiss and the clinopyroxene syenite gneiss have not norma-

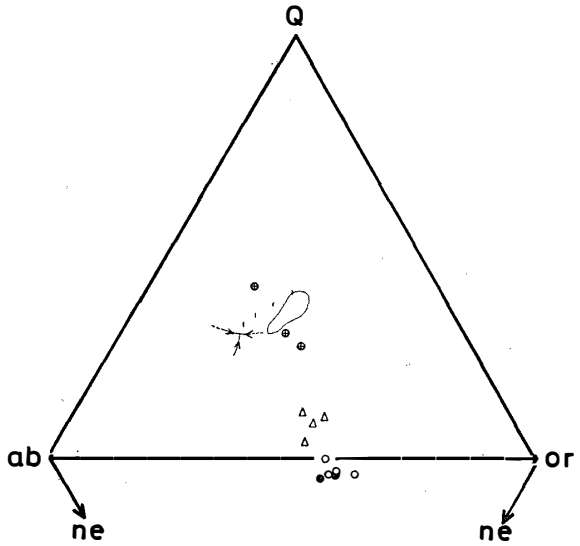

Fig. 13. Normative q-or-ab-ne diagram. The maximum concentration of normative compositions of granitic rocks is shown by closed line. Dots indicate the isobaric minimum and isobaric eutectics after TUTTLE *and* BOWEN *(1958). Symbols are the same as in Fig. 8.*

tive "q" but "ne", and they fall in the same area. As a whole, the plots of all rock types show a trend towards eutectic minimum of the system albite-orthoclase silica. There is a gap between the clinopyroxene quartz syenite gneiss and the granite gneiss. The trend towards granite gneiss represents the increase of "q", the decrease of "or" and the slight decrease of "ab".

6. 3. Discussion on the grantization

It is significant that the "or" content decreases with the progress of the granitization process, whereas the "ab" content does not change remarkably. Generally speaking, granitization is explained by the addition of both K_2O and SiO_2 (ENGEL and ENGEL, 1960; MEHNERT, 1968). However, this phenomenon occurs in the granitization of ordinary sedimentary rocks, such as pelitic rocks. In the area studied, the starting rock seems to be rich in potassium, so that it is reasonable that the granitization proceeds with the decrease of potash feldspar.

When the crust partially melts due to anatexis, the liquid should have the composition of eutectic point and this composition is poorer in K_2O than the starting rocks in this area. Therefore, if the liquid acts as the "granitizing agent", the K_2O content in the rocks formed through the granitization becomes lower from the starting rock towards granite.

7. Conclusion

In the northern Yamato Mountains, there are two groups of metamorphic rocks. One is the syenite gneiss group which was formed under the granulite facies conditions. The other is the granite gneiss group which was metamorphosed under the amphibolite facies conditions. There is a perfect transition from the syenite gneiss to the granite gneiss.

From the field occurrences and microscopic observations, it is clear that the amphibolite facies metamorphism was superimposed onto the granulite facies metamorphism. There may be a time interval between the two metamorphic episodes. That is to say, the two-pyroxene syenite gneiss activated under the amphibolite facies conditions to become the granite gneiss, *i.e.* granitization. The isotope dating of a granitic rock of the Yamato Mountains was reported as 4.57×10^8 yr. by Sr-Rb method (PICCIOTTO *et al.*, 1964). This value may correspond to the time when the granitization took place.

On the other hand, there is migmatite gneiss, the other type of the granite gneiss group, but unfortunately the relation between the migmatite gneiss and the granite gneiss is still unsolved.

There are some differences between the two-pyroxene syenite gneiss of Massif G and that of Massifs E and F. The hornblende in Massif G is brown in colour, while that of Massifs E and F is greenish. In addition to this, the two-pyroxene syenite gneiss in Massif G has plagioclase porphyroblasts which are anti-perthitic. These evidences indicate that the gneiss in Massif G retains a more primitive condition than those of Massifs E and F. The trench-like subsurface geomorphology which lies along the southern margin of Massif G seems to show the structural subsidence of Massif G. This is one of the problems which must be solved in future.

Acknowledgements

The author is deeply grateful to Professor Yoshio KATSUI who supervised the study. Dr. Kosuke ONUMA critically read the final draft of the paper. The author was benefited by discussions with his colleagues at the Department of Geology

and Mineralogy, Hokkaido University. He thanks to the members of the 14th Japanese Antarctic Research Expedition for the field program. Particularly, Mr. Kotaro YOKOYAMA was kind enough to offer the unpublished data of radio echo sounding.

Finally he wishes to extend his thanks to Professor Koshiro KIZAKI of the University of the Ryukyus for his valuable advice and encouragement.

References

AUGUSTITHIS, S. S. (1973): Atlas of the Textural Patterns of Granites, Gneiss and Associated Rock Types. Amsterdam, Elsevier, 365p.

BARTH, T. F. W. (1966): Theoretical Petrology. New York, John Wiley, 387p.

BINNS, R. A. (1965): The mineralogy of metamorphosed basic rocks from the Willyama Complex, Broken Hill District, New South Wales: Part 1. Hornblendes. Mineral. Mag., **35,** 306–326.

CHINNER, G. A. (1960): Pelitic gneisses with varying Ferrous/Ferric ratios from Glen Clova, Angus, Scotland. J. Petrol., **1,** 178–217.

COLLERSON, K. D. (1974): Descriptive microstructural terminology for high grade metamorphic tectonites. Geol. Mag., **111,** 313–318.

DEER, W. A., HOWIE, R. A. and ZUSSMAN, J. (1963): Rock forming minerals. London, Longmans, **2,** 379p; **3,** 270p.

ENGEL, A. E. J. and ENGEL, C. G. (1958, 1960): Progressive metamorphism and granitization of the major paragneiss northwest Adirondack Mountains, New York, I, II. Bull. Geol. Soc. Am., **69,** 1369–1414; **71,** 1–58.

EVANS, B. W. and LEAKE, B. E. (1960): The composition and origin of the striped amphibolites of Connemara, Ireland. J. Petrol., **1,** 337–363.

HAYAMA, Y. (1959): Some considerations on the color of biotite and its relation to metamorphism. J. Geol. Soc. Jap., **65,** 21–30.

I. U. G. S. SUBCOMMISSION ON THE SYSTEMATICS OF IGNEOUS ROCKS (1973): Classification and nomenclature of plutonic rocks, Recommendations. Neues Jahrb. Mineral. Monatsh., **4,** 149–164.

KIZAKI, K. (1965): Geology and petrography of the Yamato Sammyaku, East Antarctica. JARE Sci. Rep., Ser. C, **3,** 1–27.

LEAKE, K. (1964): The chemical distribution between ortho- and para-amphibolites. J. Petrol., **5,** 238–254.

MEHNERT, K. R. (1968): Migmatites and the Origin of Granitic Rocks. Amsterdam, Elservier, 393p.

MIYASHIRO, A. (1973): Metamorphism and Metamorphic Belts. London, George Allen & Unwin, 492p.

MOOR, A. C. (1970): Descriptive terminology for the textures of rocks in granulite facies terrain. Lithos, **3,** 123–127.

NOLAN, J. (1969): Phisical properties of synthetic and natural pyroxenes in the system diopside-hedenbergite-acmite. Mineral. Mag., **37,** 216–229.

OHTA, Y. and KIZAKI, K. (1966): Petrographic studies of potash feldspar from the Yamato Sammyaku, East Antarctica. JARE Sci. Rep., Ser. C, **5,** 1–40.

PEIKERT, E. W. (1963): Biotite variation as a guide to petrogenesis of granitic rocks in the Pre-cambrian of North-east Alberta. J. Petrol., **4,** 432–459.

PICCIOTTO, E. and COPPEZ, A. (1964): Bibliographie des mesures d'ages absolus en Antarctique. Ann. Soc. Geol. Belg., **87,** 115–128.

RAVICH, M. G. (1968): Regional metamorphism and ultrametamorphism of crystalline basement of the Antarctic and other Gondwana platforms. I.G.C. Rec. 23rd session, Geology of Pre-cambrian, 203–213.

RAVICH, M. G. (1972): Regional metamorphism of the Antarctic platform crystalline basement. Antarctic Geology and Geophysics, ed. by R.J. Adie. Oslo, Universitetsforlaget, 505–515.

RAVICH, M. G. and KAMENOV, E. N. (1975): Crystalline Basement of the Antarctic Platform. New York, John Wiley, 574p.

SHIMIZU, H., NARUSE, R., OMOTO, K. and YOSHIMURA, A. (1972): Position of stations, surface elevation and thickness of the ice sheet, and snow temperature at 10 m depth in the Mizuho Plateau—West Enderby Land area, East Antarctica, 1969-1971. JARE Data Rep., **17** (Glaciol.), 12–37.

SIMONEN, A. (1953): Stratigraphy and sedimentation of the svecofennidic, early Archean supracrustal rocks in south-western Finland. Bull. Comm. Geol. Finl., **160.**

SPRY, A. (1969): Metamorphic Textures. Oxford, Pergamon Press, 370p.

TATSUMI, T., KIKUCHI, T. and KIZAKI, K. (1964): Geology of the region around Lützow-Holmbukta and the "Yamato Mountains" (Dronning Fabiolafjella). Antarctic Geology, ed. by R. J. Adie. Amsterdam, North-Holland, 293–303.

TATSUMI, T. and KIZAKI, K. (1969): Geology of the Lützow-Holm Bay region and the 'Yamato Mountains' (Queen Fabiola Mountains). Antarctic Map Folio Series, Folio 12, Sheet 9 and 10.

TUTTLE, O. F. and BOWEN, N. L. (1958): Origin of granite in the light of experimental studies in the system $NaAlSi_3O_8$–$KAlSi_3O_8$–SiO_2–H_2O. Geol. Soc. Am., Mem., **74,** 1–153.

VAN AUTENBOER, T., MICHOT, J. and PICCIOTTO, E. (1964): Outline of the geology and petrology of the Sør-Rondane Mountains, Dronning Maud Land. Antarctic Geology, ed. by R. J. Adie. Amsterdam, North-Holland, 501–514.

VAN AUTENBOER, T. and LOY, W. (1972): Recent geological investigations in the Sør-Rondane Mountains, Belgicafjella and Sverdrupfjella, Dronning Maud Land. Antarctic Geology and Geophysics, ed. by R. J. Adie. Oslo, Universitetsforlaget, 563–571.

WONES, D. R. (1963): Physical properties of synthetic biotites on the join phlogopite-annite. Am. Mineral., **48,** 1300–1321.

YOSHIDA, M. and ANDO, H. (1971): Geological survey in the vicinity of Lützow-Holm Bay and the Yamato Mountains, East Antarctica. Nankyoku Shiryo (Antarct. Rec.), **39,** 46–54.

YOSHIDA, Y. and FUJIWARA, K. (1963): Yamato Sanmyaku no chikei (Geomorphology of the Yamato (Queen Fabiola) Mountains). Nankyoku Shiryo (Antarct. Rec.), **18,** 1–26.

(Manuscript received September 3, 1976;
Revised manuscript received June 20, 1977)